Supplemental material - Exploring the configuration space of elemental carbon with empirical and machine learned interatomic potentials

January 20, 2023

1 Verifying the general accuracy of GAP-20U+gr

In Section III.A.3 of the manuscript we present a re-trained version of the GAP-20U potential that includes additional ordered graphite configurations to more accurately capture the graphitic energy landscape in comparison to DFT. Here we show how the performance of the potential has been affected across the training set in addition to the graphite phase.

Firstly in Figure 1 we calculate, for each configuration in the training set, the difference in energy predicted by the GAP-20U, GAP-20U+gr and DFT models. These plots demonstrate that the difference between the GAP-20U and GAP-20U+gr energies are significantly reduced in comparison to the differences between the GAP-20U and DFT energies, showing that the effect of adding these ordered graphite phases is small in comparison to the accepted error between the GAP-20U and DFT models.

In Figure 2 we plot the enthalpy of select crystalline phases as a function of pressure, in order to demonstrate how the re-fitting has affected the relative stability of each structure. Though some phase boundaries are shifted in comparison to the GAP-20U, these results are largely the same and thus confirm that the additional graphite phases have not significantly affected the model's description of other phases.

2 Evaluating the graphite-diamond transition using GAP-20U+gr

Figure 3 demonstrates how the graphite-diamond transition is ascertained from nested sampling of the GAP-20U+gr potential at 20 GPa. This data shows that the new potential behaves similarly to the GAP-20U with regards to this transition, with the temperature only decreasing by around 10%.

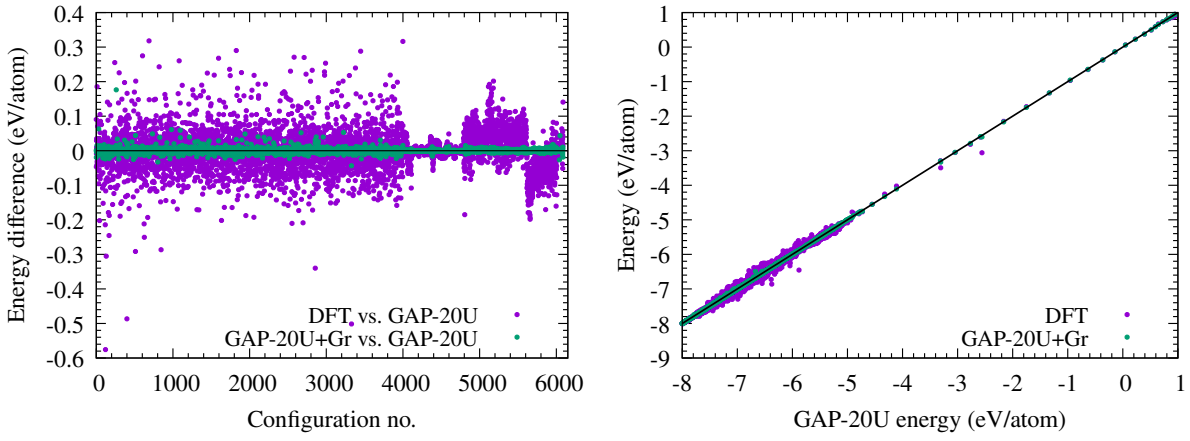

Figure 1: The difference in energies, calculated for each configuration in the training set, between the GAP-20U, GAP-20U+gr and DFT models.

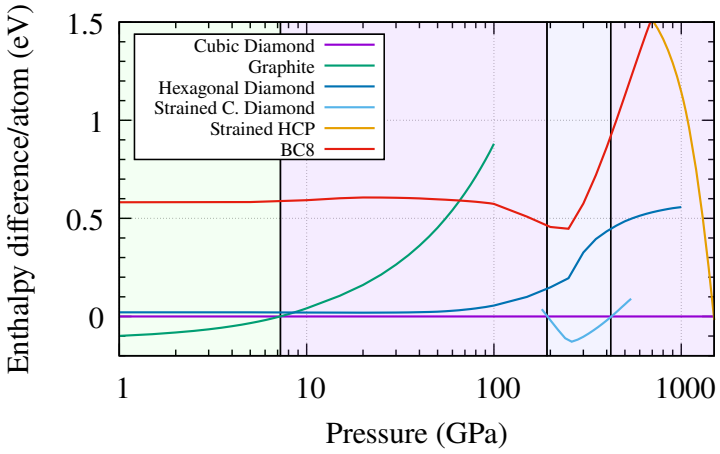

Figure 2: Enthalpy of select crystalline phases, calculated using the GAP-20U+gr model, as a function of pressure.

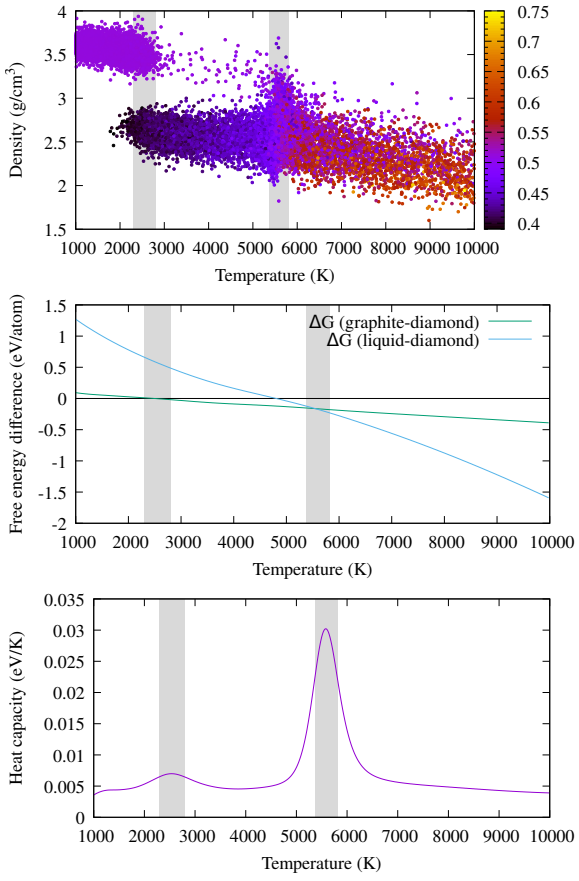

Figure 3: Nested sampling results at 20 GPa, using 16 atoms and the GAP-20U+gr potential. Top panel: density of individual configurations sampled during NS, symbols are coloured by the average Q_4 bond-order parameter of the configuration. Middle panel: Gibbs free-energy difference compared to the diamond phase. Bottom panel: The corresponding heat capacity curve. Vertical grey lines show the melting temperature, T_m and the solid-solid transition between the diamond and graphite phases, T_{DG}.

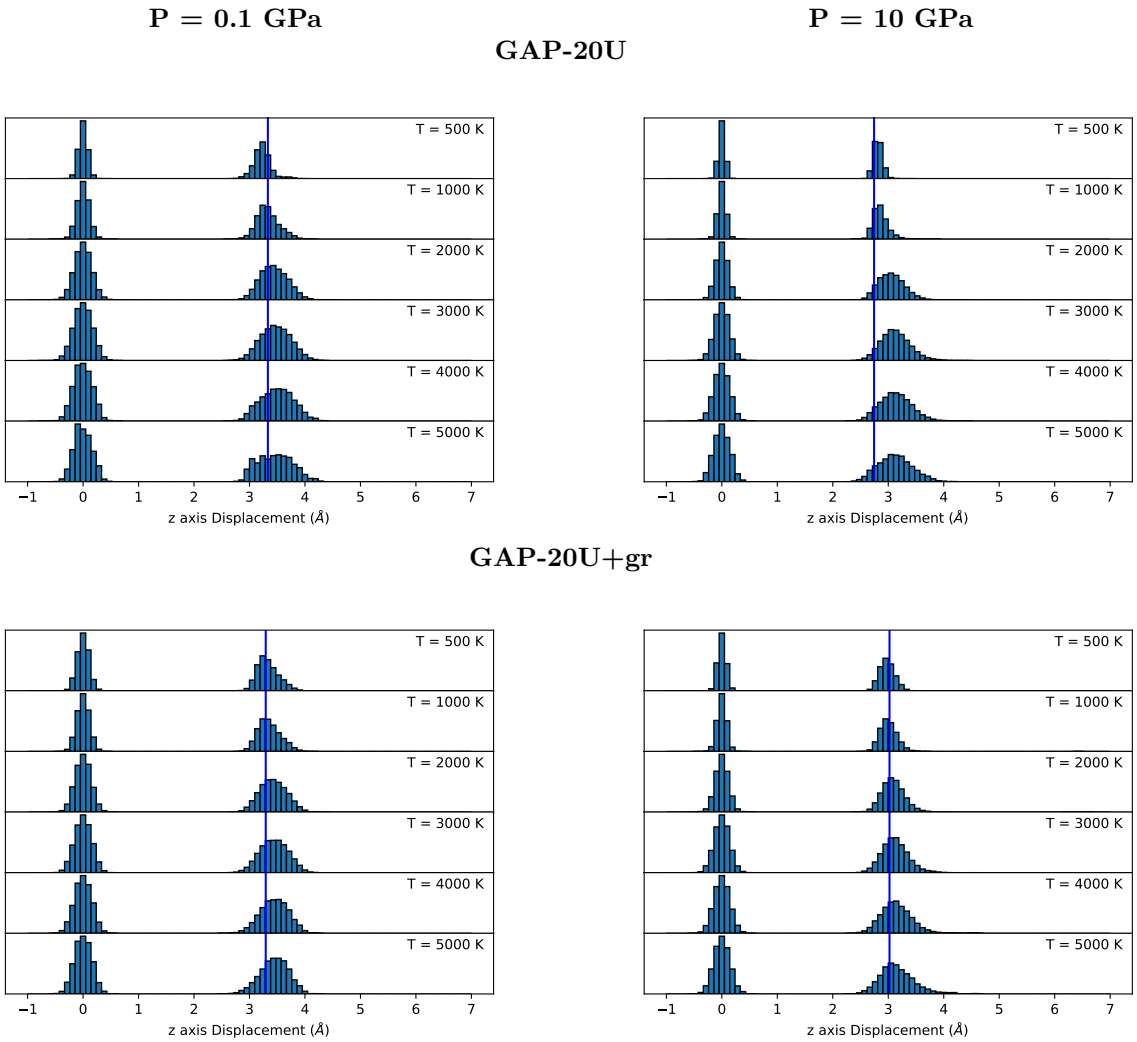

Figure 4: Distribution of the carbon atoms along the direction perpendicular to the graphite layers, calculated as the weighted average from the NS configurations, using the GAP-20U+gr potential, 16-atoms and pressures of 0.1 GPa (left) and 10 GPa (right).

3 Temperature dependence of graphite atom distributions for GAP-20U and GAP-20U+gr

In Figure 4 we show the phase space-weighted distributions of carbon atoms along the vector that is normal to the planes, calculated over a range of temperatures using the nested sampling configurations of the GAP-20U and GAP-20U+gr potentials at 0.1 and 10 GPa. Comparing the distributions of the two potentials 0.1 GPa, we see that GAP-20U+gr provides a more even distribution of layer separations at higher temperatures, due elimination of local minima with smaller separations in the graphite energy landscape. There is however still a bias toward larger separations in the GAP-20U+gr distributions due to the presence of a local minimum that could not be suppressed. Another clear improvement in the GAP-20U+gr potential can be seen at 10 GPa, where there is no phase transition from high to low separation around 2000 K.